IOPscience iopscience.iop.org

Home Search Collections Journals About Contact us My IOPscience

Growth mechanism and properties of InGaN insertions in GaN nanowires

This article has been downloaded from IOPscience. Please scroll down to see the full text article.

2012 Nanotechnology 23 135703

(http://iopscience.iop.org/0957-4484/23/13/135703)

View the table of contents for this issue, or go to the journal homepage for more

Download details:
IP Address: 200.133.194.73
The article was downloaded on 14/03/2012 at 21:54

Please note that terms and conditions apply.

Nanotechnology **23** (2012) 135703 (6pp) doi:10.1088/0957-4484/23/13/135703

Growth mechanism and properties of InGaN insertions in GaN nanowires

G Tourbot[1,2], C Bougerol[3], F Glas[4], L F Zagonel[5], Z Mahfoud[5], S Meuret[5], P Gilet[1], M Kociak[5], B Gayral[2] and B Daudin[2]

[1] CEA, LETI, MINATEC Campus, 17 rue des Martyrs, F-38054 Grenoble Cedex 9, France
[2] CEA-CNRS-UJF Group 'Nanophysique et Semiconducteurs', CEA, INAC, SP2M, NPSC, 17 rue des Martyrs, F-38054 Grenoble, France
[3] CEA-CNRS-UJF Group 'Nanophysique et Semiconducteurs', Institut Néel CNRS, 25 rue des Martyrs, F-38042 Grenoble, France
[4] CNRS-Laboratoire de Photonique et de Nanostructures, Route de Nozay, F-91460 Marcoussis, France
[5] Laboratoire de Physique des Solides, CNRS UMR8502, Université Paris-Sud XI, Bâtiment 510, F-91405 Orsay, France

E-mail: bruno.daudin@cea.fr

Received 1 February 2012, in final form 2 February 2012
Published 14 March 2012
Online at stacks.iop.org/Nano/23/135703

Abstract
We demonstrate the strong influence of strain on the morphology and In content of InGaN insertions in GaN nanowires, in agreement with theoretical predictions which establish that InGaN island nucleation on GaN nanowires may be energetically favorable, depending on In content and nanowire diameter. EDX analyses reveal In inhomogeneities between the successive dots but also along the growth direction within each dot, which is attributed to compositional pulling. Nanometer-resolved cathodoluminescence on single nanowires allowed us to probe the luminescence of single dots, revealing enhanced luminescence from the high In content top part with respect to the lower In content dot base.

(Some figures may appear in colour only in the online journal)

1. Introduction

Nanowires (NWs) of III-nitride semiconductors (GaN, AlN, InN and their alloys) are an attractive option to overcome the limitations of bidimensional heterostructures of these materials, in particular the high density of dislocations resulting from the generalized use of lattice-mismatched substrates. In contrast, NWs frequently appear to be free of structural defects. Furthermore the efficient elastic strain relaxation associated with their large aspect ratio and free surfaces [1, 2] makes the realization of mismatched heterostructures easier. Consequently, in the case of InGaN/GaN NW heterostructures, it has been found that both reduced internal electric field and increased In content could lead to the realization of light-emitting diodes in the green and yellow regions of the spectrum [3–6].

In the case of growth on bulk substrates, it is well known that InGaN deposition on GaN obeys either the Frank–van der Merwe or the Stranski–Krastanow (SK) growth mode, depending on In content [7, 8]. In the case of the SK growth mode, it has been established that the InGaN quantum dots exhibit a very small height/diameter aspect ratio, typically in the 0.05–0.1 range [7]. In contrast, in spite of recent reports on InGaN insertions in GaN NWs by several groups [5, 6, 9], the growth mode of such heterostructures is still obscure. It is the purpose of the present paper to study the formation and the structural and optical properties of InGaN insertions in GaN NWs. In particular, it will be shown that, depending on In content and diameter of the GaN NW base, the formation of three-dimensional (3D) islands may indeed reduce the elastic energy associated with InGaN–GaN lattice mismatch.

2. Experimental details

The InGaN/GaN NWs were grown by rf-plasma-assisted molecular beam epitaxy (PA-MBE) on Si(111) substrates, using a thin (2–3 nm) AlN buffer layer [10, 11]. The growth temperature was monitored in the 850–900 °C range

 © 2012 IOP Publishing Ltd Printed in the UK & the USA

by the Ga desorption method described in [12] to allow the growth of a 400–500 nm long GaN nanowire base. The temperature was then lowered to 650 °C to make possible In incorporation in the material [13]. The samples consisted of three thin InGaN insertions separated by GaN barriers grown in Ga-rich conditions. The thickness of the InGaN insertions was varied from 3 to 15 nm. The structural properties of the samples were investigated by high resolution transmission electron microscopy (HRTEM) performed in a JEOL 4000EX microscope operated at 400 kV ($C_s = 1$ mm). For this purpose, the NWs were scraped off the substrate and dispersed on Cu microscope grids covered with a holey carbon film. Energy-dispersive x-ray (EDX) spectroscopy composition analyses were performed in a field-emission scanning electron microscope (Hitachi 5500) operated in scanning transmission mode at 30 kV.

Nano-cathodoluminescence (nanoCL) was performed at 150 K in a Vacuum Generators HB-501 scanning transmission electron microscope operating at 60 kV. The whole set-up including an in-house high throughput CL system is described in [14]. In brief, an electron beam, about 1 nm in size, is scanned on the sample with typically nanometer steps. At each position of the scan, both a CL spectrum and a high angular annular dark field (HAADF) signals are recorded. At the end of the scan, this results in the parallel acquisition of both a CL spectral image and an HAADF image. This allows for a direct, pixel per pixel, comparison of the spectral and structural information. The spatial resolution is sample-dependent, the best spatial resolution reported being close to one nanometer [14].

3. Results

The HRTEM images of two GaN NWs, each containing three InGaN insertions of approximately equal thickness (respectively 15 and 6 nm), are presented in figures 1(a) and (b). In both cases, the InGaN insertions exhibit a truncated pyramidal morphology, with well-defined facets. Such a shape is comparable to that of InGaN quantum dots grown on bidimensional (2D) GaN layers, namely with inclined (1–10×) side facets and a flat (0001) top facet [15]. However, the aspect ratio of the present insertions is significantly higher than usually observed for InGaN quantum dots grown on 2D GaN substrates [15, 7]. Indeed, the angle between the (0001) planes and the side facets reaches about 45° for 8 nm thick insertions (not shown here) and 55° for the 15 nm thick ones, compared with 32° for the (1–103) facets of QDs grown by metal–organic chemical vapor deposition (MOCVD) on a GaN template [15]. Such an increase in aspect ratio with increasing volume was previously observed for InAs [16] and InGaN/GaN quantum dots [17] grown on bulk substrates. More generally, as theoretically predicted by Daruka *et al* [18], this behavior is typical of strain-driven 3D islanding. Therefore, it seems that, in spite of the widely acknowledged notion that strain is easily accommodated in nanowire heterostructures [2, 19], the remaining elastic energy might still be sufficient to influence strongly the morphology of InGaN/GaN insertions. Finally, the enlargement shown in figure 1(c) reveals the absence of wetting layer at the base of the insertion, which tends to suggest that, if it is actually strain-induced, the growth of InGaN islands on top of NWs possibly obeys the Volmer–Weber mode rather than the Stranski–Krastanow mode.

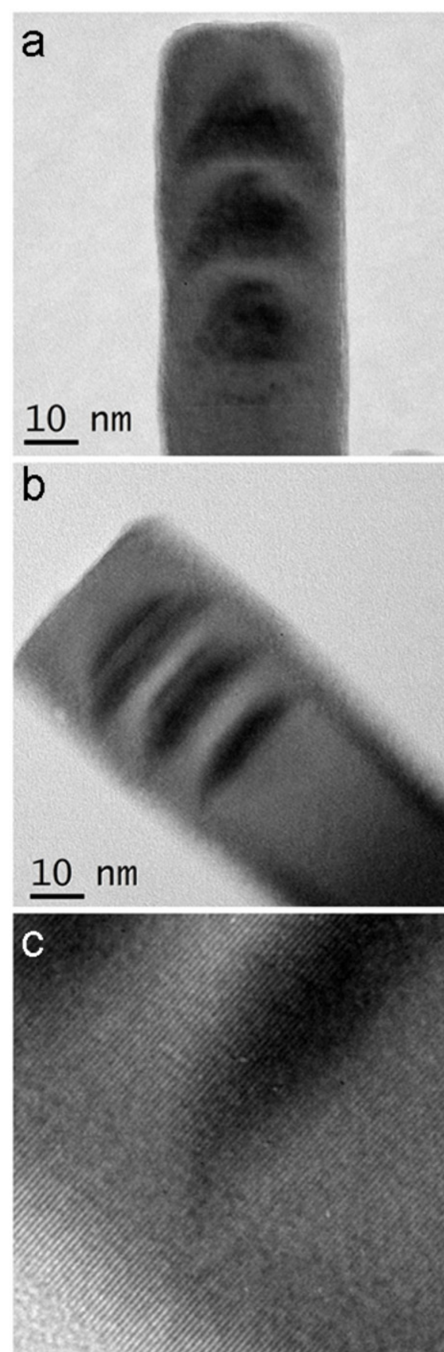

Figure 1. HRTEM images of InGaN insertions (dark) in a GaN nanowire, of nominal thickness 15 nm (a) and 6 nm (b), respectively. (c) Zoom on the left side of the bottom insertion from (b), revealing the absence of a wetting layer.

To get more insight into the strain relaxation mechanism and to check that it could indeed induce the island growth of the InGaN deposit, we calculated the total energy of a GaN NW on top of which is deposited an InGaN island. As a

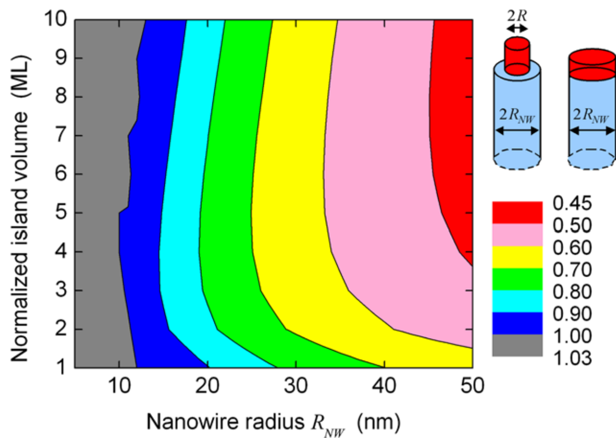

Figure 2. Map of the minimum total energy of the system formed by a cylindrical island located at the center of the top facet of a semi-infinite cylindrical nanowire of radius R_{NW}, as a function of the island volume (expressed in monolayers (MLs) of radius R_{NW}). The energy is found by minimizing the sum of the elastic and surface energies of the whole system at variable island radius $R \leq R_{\mathrm{NW}}$ and constant island volume. The energy is normalized to that of the system with the same island volume deposited as a disc of radius R_{NW}. The relative lattice mismatch of the insertion is 4% and its sidewall surface energy 1.8 J m^{-2}.

first approximation, we considered a rotationally symmetric system consisting of a long cylindrical NW foot of radius R_{NW} topped by an axial cylindrical island of radius $R \leq R_{\mathrm{NW}}$. The total energy was taken as the sum of the elastic energy corresponding to the coherent relaxation of the whole system (calculated in the framework of isotropic elasticity by using a finite element software) and of the surface energy of the island sidewalls. This energy was then compared to that of an InGaN layer of equal volume and In content covering homogeneously the whole top facet of the nanowire ($R = R_{\mathrm{NW}}$). The calculation was performed for a wide range of nanowire radii, InGaN volumes and lattice mismatches, and the radius of the island was allowed to vary freely.

The calculated energy of the most favorable InGaN island configuration, divided by that of the homogeneous InGaN disc configuration, is displayed in figure 2 for an InGaN/GaN lattice mismatch of 4%, i.e. an In content of about 35% in InGaN. Interestingly, in the range of NW radii and island volumes considered, the total energy of the structure can be reduced by up to 55%, if the InGaN does not cover the whole top surface but instead forms as a cylinder of smaller diameter. In addition, we considered the possibility of island formation at the periphery of the top facet. This configuration may be even more favorable than the axial one, but only for very small NW radii. In the limits of the cylindrical NW and island shapes of this simple model, we thus conclude that the strain relaxation afforded by the nanowire geometry does not systematically promote pseudo-2D growth over island nucleation on the nanowire top, since the latter can lead to an even reduced elastic energy [20]. Note that the strain-driven formation of axial islands considered here differs fundamentally from that of lateral islands or corrugations on the sidewalls of NWs, as observed experimentally [21] and studied theoretically [22] in the past.

The In composition of the insertions was measured by EDX spectroscopy. Figure 3(a) shows a typical profile of the In content obtained from a linescan across the successive insertions in the growth direction, as indicated in the corresponding image (figure 3(b)). Since the analysis was carried out without standards and because the dot geometry implies that the volume analyzed includes both GaN and InGaN, the compositions obtained cannot be considered as absolute values. However, two main features are clearly observed. First, the three insertions present an asymmetrical profile with a much sharper InGaN/GaN interface at the top of the dot than the GaN/InGaN one at the base. Second, the first insertion is different from the two others, with a lower In content as well as a lower height (as also visible in figure 1).

From these data, it first appears that In incorporation is hindered close to the base of the dots, and most favorable at the top of them. We attribute this progressive increase of In content to a compositional pulling effect [23]: the

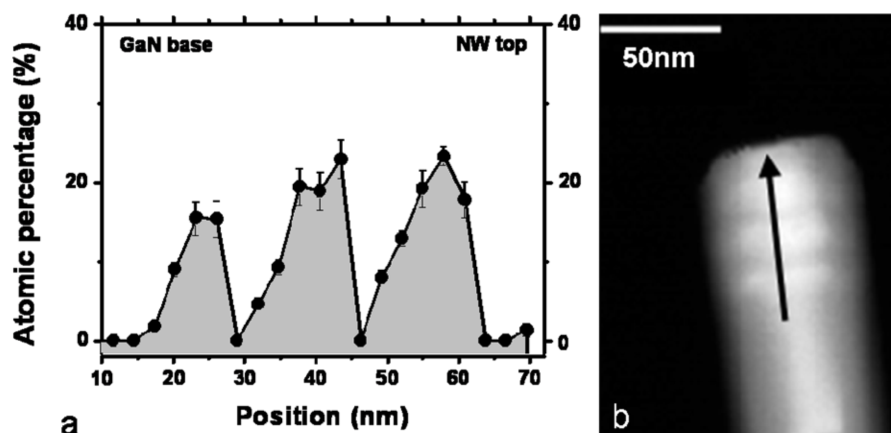

Figure 3. In content profile (a) obtained from an EDX linescan along a single GaN nanowire containing three InGaN dots, as indicated by the black arrow in (b).

incorporation of In in the dots is limited by the strain state, leading to a higher In content at the top of the dots where strain is efficiently relaxed due to the 3D nature of the island [24–26]. Consistent with such a speculation, the lower volume and In content of the first dot is tentatively attributed to differences in the underlying substrate (in this case, strain-free GaN or GaN barrier with an underlying InGaN island), leading to a lower In incorporation in the first dot due to compositional pulling. Since it is generally assumed that Ga adatoms are incorporated preferentially with respect to In adatoms [27, 28], we then suggest that the increased In incorporation in the upper dots of the stacking contributes to the increase in dot height.

The optical properties of InGaN insertions in GaN NWs were studied by performing nanoCL experiments on single GaN NWs containing three 15 nm thick InGaN insertions. Given the insertion thickness and the 10 nm thick barriers, that are much larger than the probe size, the thickness of the wire, that did not induce appreciable broadening of the electron probe, and a low diffusion length of charge carriers (see the discussion below), the spatial and spectral resolution of the set-up allowed us to probe each individual dot. Figure 4 (a) presents the STEM–HAADF image of such a NW, showing the three InGaN insertions as brighter zones. Figure 4(b) shows a spatial/wavelength mapping of the CL emission spectrum in the nanowire growth direction superimposed on the STEM–HAADF intensity profile. Typical spectra extracted at the positions indicated on the HAADF image are displayed in figure 4(c). One can see a strong 495 nm emission originating from the top insertion as well as a lower intensity 487 nm emission originating from the first insertion. The second dot does not emit any observable signal. That not all inclusions emit light was observed on almost all investigated NWs, although there was no clear pattern as to which insertion would luminesce. It is not clear at this stage if the inhibition of light emission from one or two insertions of the stacking is due to non-radiative recombination on structural defects or to another non-radiative mechanism. The two identified emissions peak in intensity when the electron beam excites the upper region of each insertion. Such a behavior was seen in about half of the inclusions investigated.

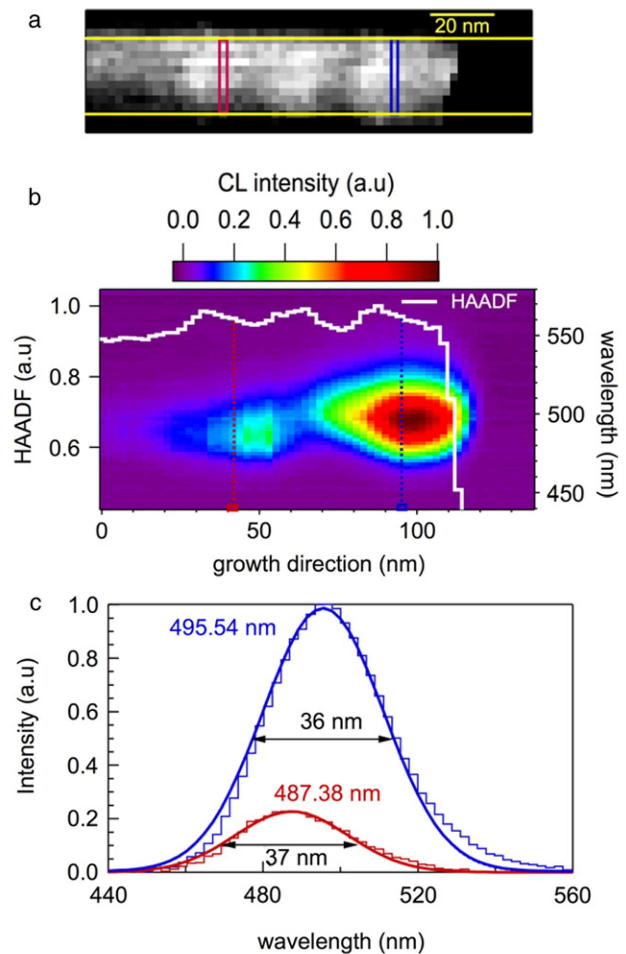

Figure 4. (a) STEM–HAADF micrograph of a single InGaN/GaN nanowire. The three InGaN insertions appear as brighter areas. (b) CL signal integrated between the horizontal lines in figure 1(a): the horizontal axis is the spatial position along the wire growth direction, the vertical axis is the emission wavelength. The intensity is color-coded. Superimposed is the STEM–HAADF intensity profile integrated on the same area; the dotted lines correspond to the positions of the colored rectangles in (a). (c) Representative spectra extracted from the two emitting inclusions as indicated by the dotted lines in (b).

The analysis of figure 4 leads to several conclusions. We first note that, despite the strong In composition gradient measured by EDX (figure 3), there is barely any spectral shift within each insertion in the nanoCL spectra. This shows that the radiative recombinations always take place at the same location within the insertion, whatever the nanoCL exciting spot location in the insertion. From the spectral position of the CL peak (around 490 nm), one can infer an In composition around 20% [29] at the position of radiative recombination. Then, the comparison with the EDX data shows that the radiative recombination takes place near the top of the insertion. The second important point is that the nanoCL signal varies strongly in intensity with the beam position along the nanowire axis at scales smaller than the thickness of an insertion. This shows that the excitation volume is smaller than the insertion volume, and that the diffusion length of cathodo-created carriers is also smaller than the insertion thickness (15 nm in this case). Because the diffusion length is smaller than the inclusion length, we should expect for a given inclusion some recombinations at different wavelengths corresponding to lower In content, especially when the beam hits the bottom of the inclusion, which is not the case. This means more precisely that, for carriers created away from the radiative recombination zone, non-radiative recombinations only occur on the diffusion/relaxation path towards the upper part of the insertion. It thus appears that the upper part of each insertion is much more radiative than the lower part where strong non-radiative recombinations occur. While we do not have an explanation for these strong non-radiative recombinations, we note that they occur in the low In content InGaN, which is in contrast with two-dimensional InGaN films for which the high In content InGaN is less radiative [29]. In two-dimensional films, the precise mechanism responsible for non-radiative

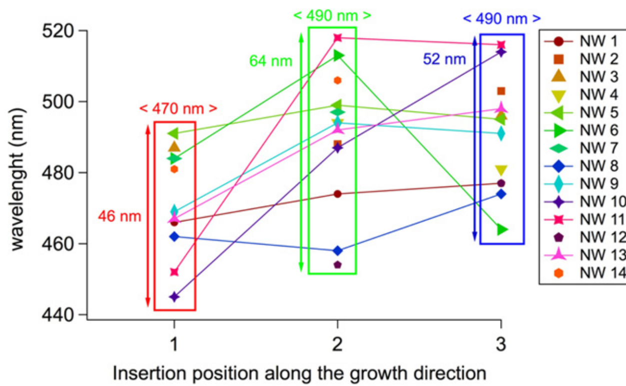

Figure 5. Wavelength measurement of the three inclusions along the growth direction for 14 different nanowires. Missing points correspond to non-emitting inclusions. Mean wavelengths (in brackets) and wavelength ranges are given for each type of inclusion.

recombinations in high In content InGaN is not clear yet, one possible explanation being an increase in point defect density in high In content InGaN [29]. Here, one can also speculate on the effect of the reduced thickness and the reduced charge carrier confinement (due to a smaller gap contrast) of the lateral GaN shell towards the base of the dots. For InGaN grown on GaN nanowires, it is not surprising that the InGaN crystal growth mechanism differs from the two-dimensional situation, in particular due to the progressive strain relaxation of the insertion along the growth axis.

We deduce from the nanoCL study that, in this system, diffusion and non-radiative recombinations can be probed at very short scales (<5 nm). While some InGaN insertions do not luminesce at all, those that luminesce appear to be strongly non-radiative in the lower In content InGaN and to be most efficient in the upper part where the highest In content is found.

The nanoCL also allows one to probe the peak emission wavelength for each insertion in various nanowires. These are summed up in figure 5. It has to be noticed that the relative peak emission wavelengths of the different insertions in a given NW can be shifted by several tens of nanometers, thus contributing to the wide emission already observed in such systems [30]. In agreement with the lower In content in the first dot common to all the NWs studied by EDX, the average CL emission wavelength of the first dot is shorter than the average emission wavelength of the following dots. However, it is clear from figure 5 that some of the individual NWs do not follow this general trend.

4. Discussion and conclusion

As a summary, the theoretical results reported above establish that, in a wide range of diameter and lattice mismatch, InGaN deposited by PA-MBE on top of GaN NWs should adopt an island shape, the formation of such islands being energetically more favorable than that of discs fitting the NW diameter. In the case of InGaN/GaN stackings on planar substrates, the 3D island strain relaxation combined with different diffusion coefficients for Ga and In adatoms have been found to promote inhomogeneous In distribution. For high enough In content, a plastic strain relaxation has been observed in the case of InGaN NW sections grown on GaN NWs while for lower In content it has been found that InGaN NW sections deposited on top of a GaN NW spontaneously formed a core/shell structure [3]. Consistent with the results reported here, it has been proposed that the growth of such a self-assembled InGaN/GaN core/shell structure was triggered by the formation of an In-rich 3D island and subsequent strain-assisted adatom diffusion [3]. In the same way, the growth of GaN barriers on pre-existing three-dimensional InGaN islands should lead to a lateral encapsulation [31], potentially minimizing the surface recombination of carriers.

Recently, a detailed microphotoluminescence study of InGaN/GaN NW LEDs has put in evidence a significant wavelength dispersion, each nanoLED emitting at a different wavelength [4]. As shown by Sekiguchi *et al* [32], it is expected that the convolution of impinging In flux with the NW diameter fluctuations and NW density distribution will eventually result in fluctuations of the total In content from one NW to another. On the nanoscopic scale, nanoCL experiments reported in the present work show that the emission wavelength of different dots in a single NW can be markedly different, possibly due to different strain relaxation levels. As emission emanates mostly from the upper part of the dots, i.e. from the region with higher In content, this suggests that strain pulling also partially controls the InGaN dot emission wavelength by contributing to carrier localization. There is therefore an intrinsic tendency to polychromaticity in a close stacking of InGaN QDs in a GaN NW, which contributes to the microscopic polychromaticity observed in [4]. As strain relaxation will vary with the diameter of the GaN base, these effects can, in our view, also reflect the NW diameter dispersion and therefore contribute to the microscopic polychromaticity. Moreover, the nanoCL study shows that strong non-radiative recombinations occur in the InGaN insertions: while some insertions do not luminesce at all, in half of the insertions the luminescence is quenched in the lower part where less In is incorporated. At this stage, one can only speculate on the non-radiative recombination process occurring in the insertions, which requires further studies. At any rate, this particular study highlights the originality of the nanoCL set-up which allows one to draw precise conclusions on the diffusion processes and non-radiative recombinations at unprecedented scales (less than 5 nm).

In conclusion, we have shown that, provided the lattice mismatch and the base diameter are high enough, InGaN grown on GaN nanowires preferentially forms 3D islands for minimizing the elastic energy. Consistent with these theoretical predictions, it has been inferred from experimental data that both morphology and In content distribution in InGaN islands are closely related to the elastic strain relaxation mechanism. These features are expected to be general, whatever the growth technique used to elaborate InGaN/GaN NW heterostructures, be it MBE or MOCVD. While on the one hand the non-radiative recombination put in evidence in this work is certainly detrimental for the realization of devices, on the other hand the self-encapsulating growth mode should be favorable as the active regions should experience reduced surface effects.

Acknowledgments

This work was partly supported by the French National Research Agency (ANR) through Carnot funding and through the Nanoscience and Nanotechnology Program (Project BONAFO no. ANR-08-NANO-031-01). Part of this work has been funded through the METSA network. We also acknowledge the technical assistance of Y Curé for operating the MBE machine.

References

[1] Ertekin E, Greaney P A, Chrzan D C and Sands T D 2005 *J. Appl. Phys.* **97** 114325
[2] Glas F 2006 *Phys. Rev.* B **74** 121302(R)
[3] Tourbot G, Bougerol C, Grenier A, Den Hertog M, Sam-Giao D, Cooper D, Gilet P, Gayral B and Daudin B 2011 *Nanotechnology* **22** 075601
[4] Bavencove A-L, Tourbot G, Garcia J, Désières Y, Gilet P, Levy F, André B, Gayral B, Daudin B and Dang L S 2011 *Nanotechnology* **22** 345705
[5] Kikuchi A, Kawai M, Tada M and Kishino K 2004 *Japan. J. Appl. Phys.* **43** L1524
[6] Guo W, Banerjee A, Bhattacharya P and Ooi B S 2011 *Appl. Phys. Lett.* **98** 193102
[7] Adelmann C, Simon J, Feuillet G, Pelekanos N T and Daudin B 2000 *Appl. Phys. Lett.* **76** 1570
[8] Waltereit P, Brandt O, Ploog K H, Tagliente M A and Tapfer L 2002 *Phys. Rev.* B **66** 165322
[9] Knelangen M, Hanke M, Luna E, Schrottke L, Brandt O and Trampert A 2001 *Nanotechnology* **22** 365703
[10] Largeau L, Dheeraj D L, Tchernycheva M, Cirlin G E and Harmand J C 2008 *Nanotechnology* **19** 155704
[11] Songmuang R, Landré O and Daudin B 2007 *Appl. Phys. Lett.* **91** 251902
[12] Landré O, Songmuang R, Renard J, Bellet-Amalric E, Renevier H and Daudin B 2008 *Appl. Phys. Lett.* **93** 183109
[13] Adelmann C, Langer R, Feuillet G and Daudin B 1999 *Appl. Phys. Lett.* **75** 3518
[14] Zagonel L F *et al* 2011 *Nano Lett.* **11** 568
[15] Bai J, Wang Q, Wang T, Cullis A G and Parbrook P J 2009 *J. Appl. Phys.* **105** 053505
[16] Saito H, Kishi K and Sugou S 1999 *Appl. Phys. Lett.* **74** 1224
[17] Gangopadhay S, Schmidt Th, Einfeld S, Yamaguchi T, Hommel D and Falta J 2007 *J. Vac. Sci. Technol.* B **25** 791
[18] Daruka I, Tersoff J and Barabási A L 1999 *Phys. Rev. Lett.* **82** 2753
[19] Raychaudhuri S and Yu E T 2006 *J. Appl. Phys.* **99** 114308
[20] Glas F *et al* 2012 in preparation
[21] Pan L, Lew K-K, Redwing J M and Dickey E C 2005 *Nano Lett.* **5** 1081
[22] Schmidt V, McIntyre P C and Gösele U 2008 *Phys. Rev.* B **77** 235302
[23] DeCrémoux B 1982 *J. Physique Coll.* **43** C5–19
[24] Medhekar M V, Hegadekatte V and Shenoy V B 2008 *Phys. Rev. Lett.* **100** 106104
[25] Schulli T U *et al* 2009 *Phys. Rev. Lett.* **102** 025502
[26] Stringfellow G B 2010 *J. Cryst. Growth* **312** 735
[27] Storm D F 2001 *J. Appl. Phys.* **89** 2452
[28] Storm D F, Adelmann C and Daudin B 2001 *Appl. Phys. Lett.* **79** 1614
[29] Kudrawiec R, Siekacz M, Krysko M, Cywinski G, Misiewicz J and Skierbiszewski C 2009 *J. Appl. Phys.* **106** 113517
[30] Chang Y L, Wang J L, Li F and Mi Z 2010 *Appl. Phys. Lett.* **96** 013106
[31] Nguyen H P T, Zhang S, Cui K, Han X, Fathololoumi S, Couillard M, Botton G A and Mi Z 2011 *Nano Lett.* **11** 1919
[32] Sekiguchi H, Kishino K and Kikuchi A 2010 *Appl. Phys. Lett.* **96** 231104